Supporting Information for

Synergistic performance of sub-nanoscopic cobalt and imidazole grafted in porous organic polymer for CO_2 fixation to cyclic carbonates under ambient pressure without co-catalyst

Jeet Chakraborty,[‡a,b] Ipsita Nath, [‡*,a,b] Shaoxian Song,[b] Chih-Ming Kao[e] and Francis Verpoort*[a,c,d]

[a] *Laboratory of Organometallics, Catalysis and Ordered Materials, State Key Laboratory of Advanced Technology for Materials Synthesis and Processing, Center for Chemical and Material Engineering, Wuhan University of Technology, Wuhan 430070, China.*

[b] *School of Resources and Environmental Engineering, Wuhan University of Technology, Wuhan 430070, China.*

[c] *Centre for Environmental and Energy Research, Ghent University Global Campus, 119 Songdomunhwa-Ro, Yeonsu-Gu, Songdo, Incheon 406-840, South Korea.*

[d] *National Research Tomsk Polytechnic University, Lenin Avenue 30, Tomsk 634050, Russia.*

[e] *Institute of Environmental Engr., National Sun Yat-Sen University, Kaohsiung, Taiwan.*

‡ These authors have contributed equally

Corresponding authors

*Ipsita Nath.

E-mail address: ipsita.nath@hotmail.com

*Francis Verpoort.

E-mail address: francis.verpoort@ghent.ac.kr

1. Materials.

All chemicals and solvents were purchased from Aladdin China and used without further purification.

2. Physical measurements.

Infrared Spectroscopy. FTIR were recorded on a Bruker Vertex 80V.

Gas sorption analysis. The adsorption-desorption isotherms were analyzed by Micrometrics instrument (ASAP 2020) using ultrapure N_2 (99.999%) at 77.3K. Samples were degassed at 120 ^oC for 6h at vacuum prior analysis. Surface area values were calculated using Brunauer-Emmett-Teller (BET) method at $0.003 < P/P_0 < 0.05$ range. Pore size distributions were calculated from N_2 sorption isotherms using the nonlocal density functional theory (NLDFT).

Morphology study. The morphology study was conducted by a S4800 field emission scanning electron microscope (FESEM, Hitachi, Japan). TEM analysis was carried out in a Philips CM20 microscope at 200 kV. Imaging and diffraction of the structure was performed at low electron dose for minimizing beam damage to the sample.

X-ray photoelectron spectroscopy (XPS). The binding energies of the elements present in the polymer were measured by XPS on Thermo Fisher ESCALAB 250Xi.

X-ray Powder Diffraction (XRD). Powder XRD analysis were performed on Bruker D8 Advance diffractometer with a copper Kα radiation source (λ= 1.54056 Å) at 40 kV and 45 Ma with 5 ^{o}/sec scanning speed.

Inductively coupled plasma optical emission spectroscopy (ICP-OES). The content of Co was estimated using a Varian VISTAMPX.

Temerature programmed desorption (TPD). The analyses were performed using the AutoChem II 2920 Chemisorption Analyzer from Micromeritics. TPD experiment was carried out under He (10 ml/min) at a constante rate of 10 ^{0}C/min.

Gas Chromatography (GC). The cyclic carbonate products were analysed by GC (Agilent) with a HP-5 column and a flame ionization detector using methanol as the eluent.

3. Methods.

3.1. Synthesis of ZIF-67-Br

A cobalt nitrate hexahydrate (291 mg) solution in methanol (30 mL) was added to a conical flask charged with 2-methyl imidazole (493 mg), and 4-bromo-2-methyl imidazole (322 mg) in methanol (30 mL). The mixture was then stirred at room temperature for 24 h. The purple solid products obtained were seperated by centrifugation, washed with methanol and dried under vacum for 12 h to obtain pure ZIF-67-Br.

3.2. Synthesis of Co-POP

In a round bottom flask charged with 1,3,5-triethynylbenzene (125.9 mg) and 1,4-dibromobenzene (113.5 mg), ZIF-67-Br (30 mg), was added $Pd(PPh_3)_4$ (20 mg), CuI (6 mg), DMF (30 ml) and Et_3N (10 ml). The reaction mixture was degassed with Ar and heated at 90 ^oC for 5 days. After the reaction was completed the yellowish product was washed throrougly and successively wih DMF, water, ethanol, 0.1 M acetic acid solution in ethanol, and acetone, followed by a treatment with methanol and acetone in a soxhlet for 24 hour and dried over vaccum.

3.3. Synthesis of Im-grafted Co-free POP

The Co-POP obtained by aforementioned method was impregnated successively in 5M HCl solution in ethanol followed by 3M NaOH solution in ethanol, and finally in normal ethanol each for 30 min. The suspension of the polymer in ethanol (acidic, basic or 'neutral') was contenuously stirred at 800 rpm during this period to get rid of the Co, and any additional impurities. Finally the compound was dried in vaccum to obtain metal free Im-grafted POP.

3.4. Synthesis of Co and Im free POP

The material was prepared following an identical protocol as Co-POP only in the absence of ZIF-67-Br.

3.5. General procedure for CO_2 cyclization reaction from Epoxide.

In a typical reaction procedure, an autoclave was charged with 20 mg of Co-POP and 8 mmol of respective epoxide. Then the autoclave was sealed and purged with CO_2 gas for 5 minute. The gas outlet was closed and reaction mixture was stirred at 100 ^oC for 8 hours under 1 bar pressure. After the reaction was finished the reactor was cooled down and the pressure was slowly released, the catalyst was separated by filtration. The products were analyzed by gas chromatography.

3.6. Calculation of Turnover Frequency (TOF).

TOFs were calculated as mmole of substrates formed per mmole of catalyst in unit time. For this calculation, the mmole of Co was considered as the “catalyst”.

4. Characterizations and catalytic data.

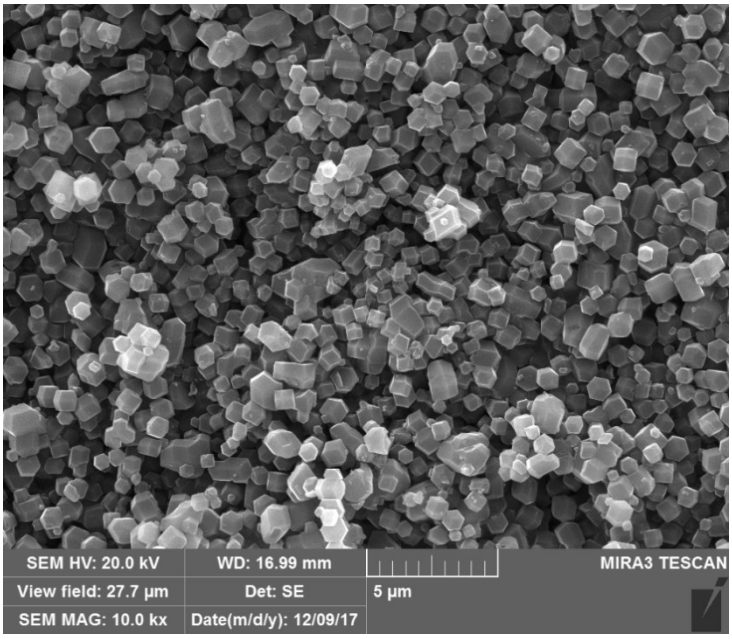

Fig. S1. FESEM image of ZIF-67-Br.

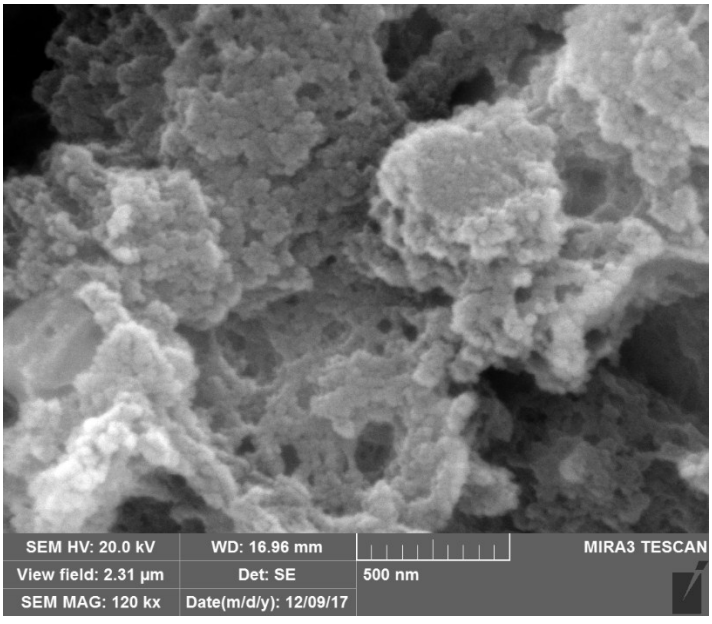

Fig. S2. FESEM image of Co-POP.

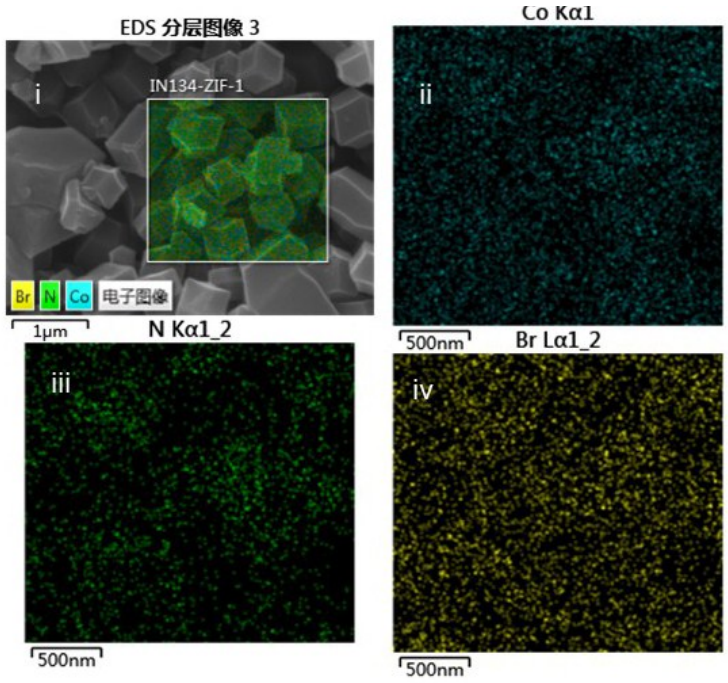

Fig. S3. EDS mapping of ZIF-67-Br; i) selected region for mapping, ii) Co, iii) N and iv) Br distribution.

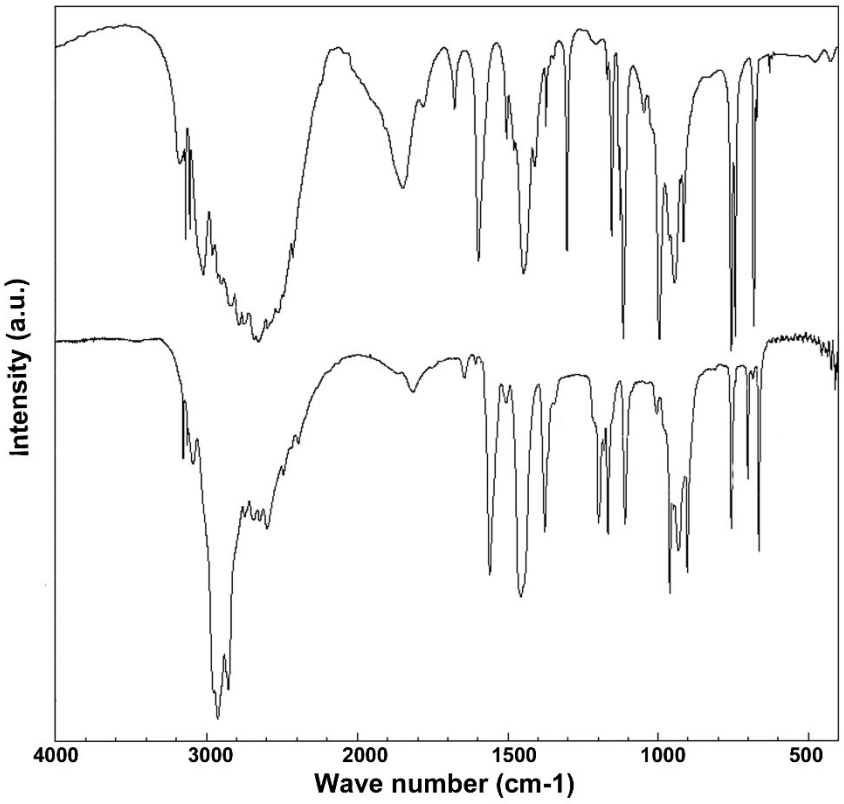

Fig. S4. Comparative FTIR spectra of 2-MIm (top) and 4-Br-2-MIm (bottom).

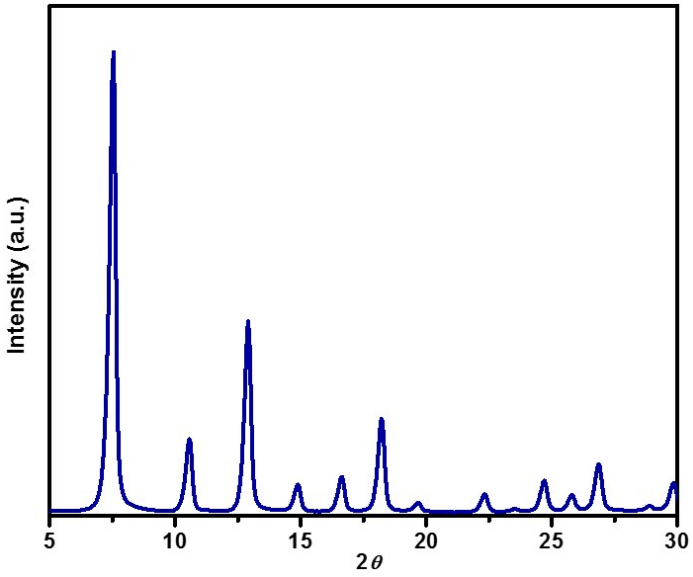

Fig. S5. XRD of ZIF-67-Br.

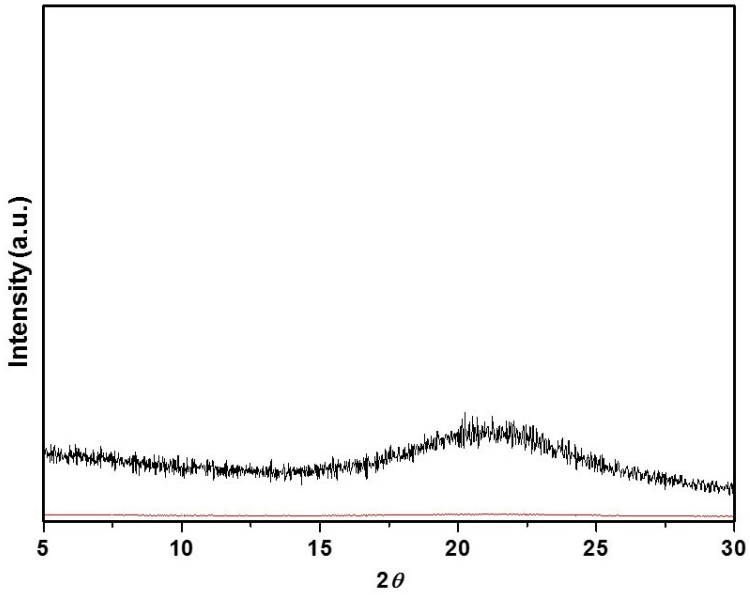

Fig. S6. XRD of Co-POP.

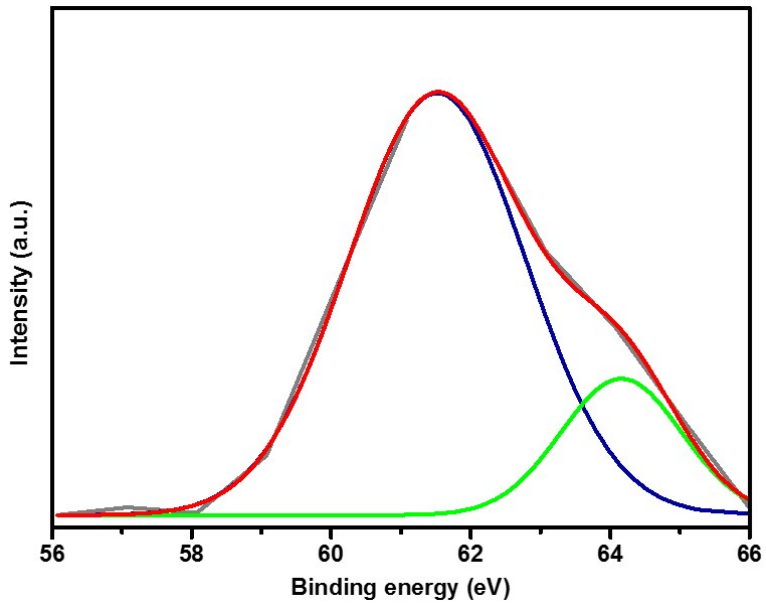

Fig. S7. Co3p HR-XPS spectra of Co-POP.

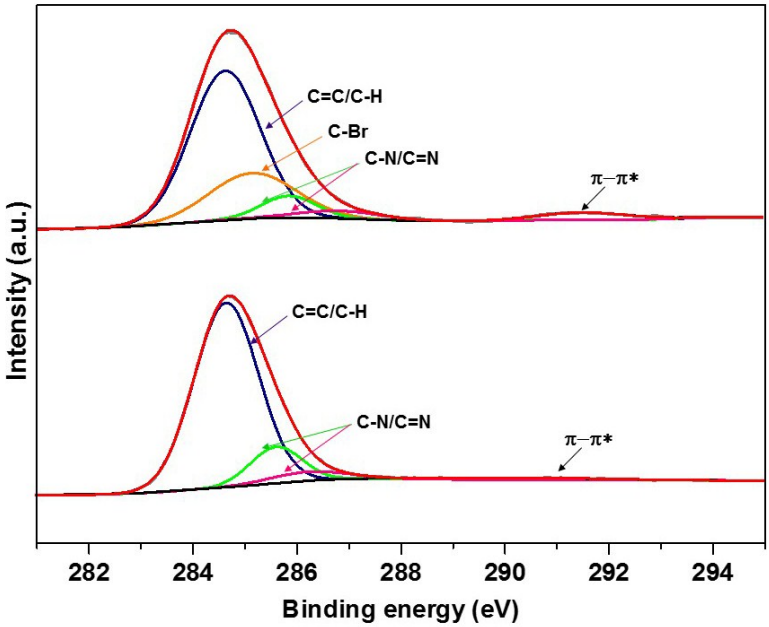

Fig. S8. C1s HR-XPS spectra of ZIF-67-Br (top) and Co-POP (bottom).

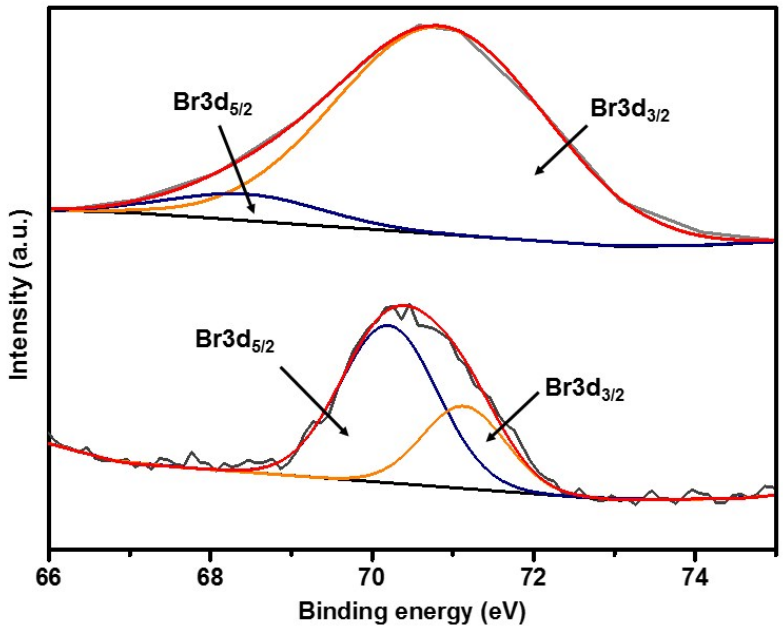

Fig. S9. Br3d HR-XPS spectra of ZIF-67-Br (top) and Co-POP (bottom).

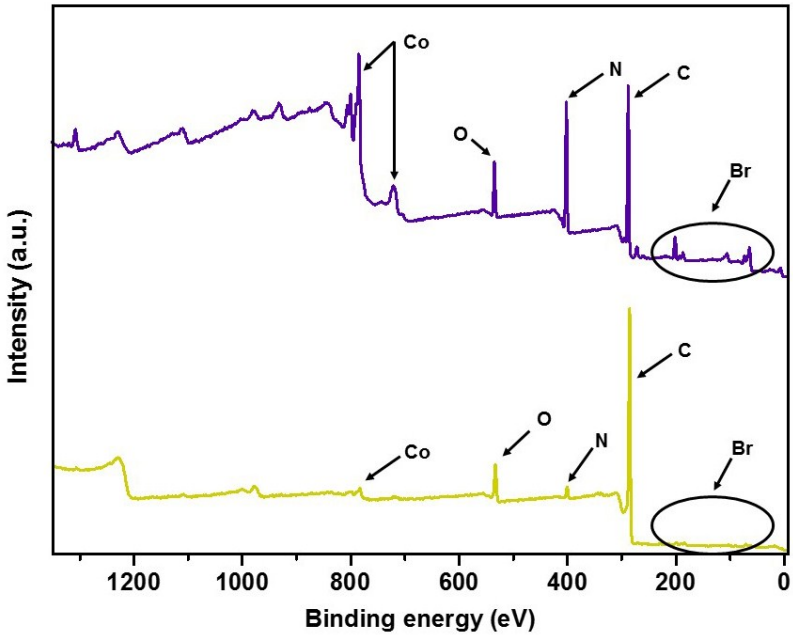

Fig. S10. XPS total survey of ZIF-67-Br (top) and Co-POP (bottom).

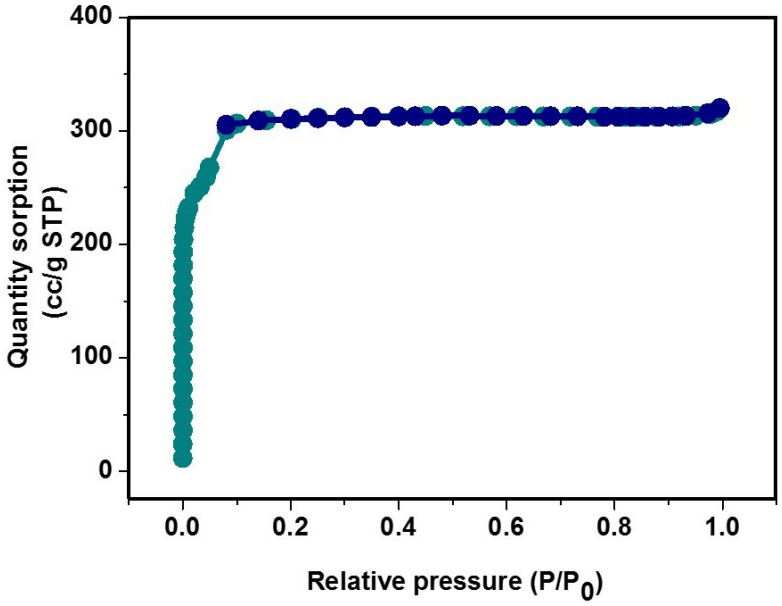

Fig. S11. N_2 sorption plot of ZIF-67-Br.

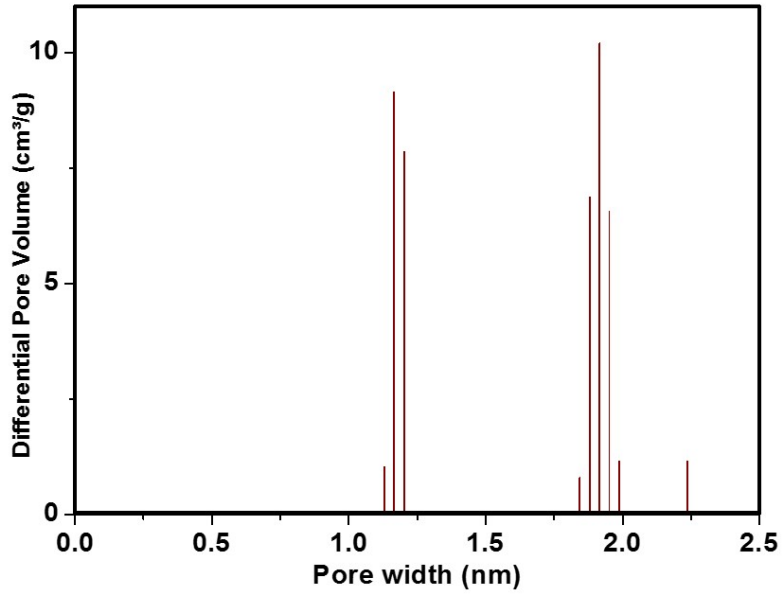

Fig. S12. NLDFT porosity distribution plot of ZIF-67-Br.

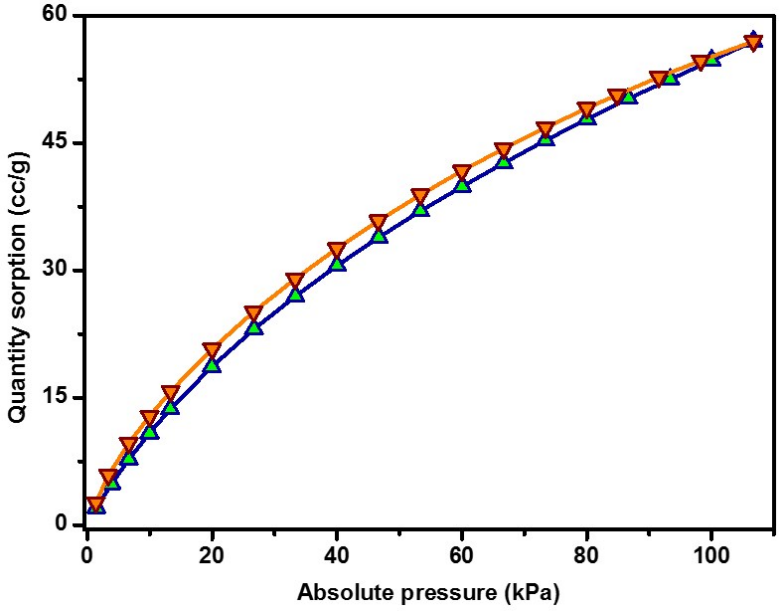

Fig. S13. CO_2 adsorption desorption pattern of Co-POP measured at 298K.

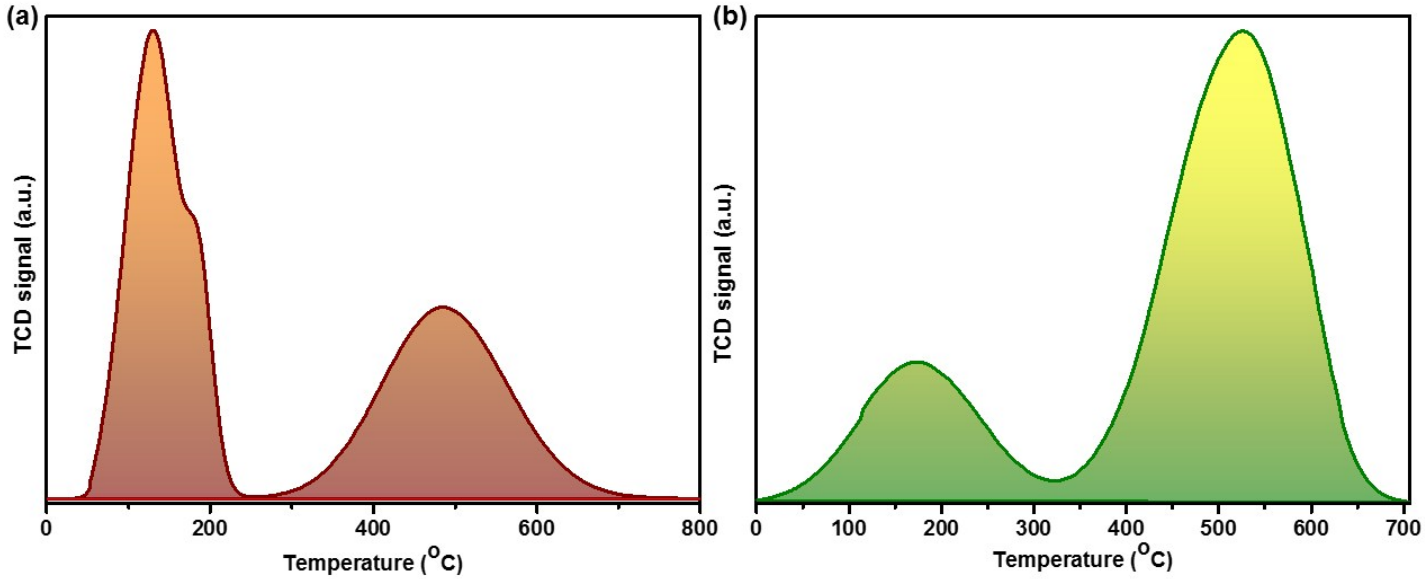

Fig. S14. (a) CO_2-TPD and (b) NH_3-TPD pattern of Co-POP.

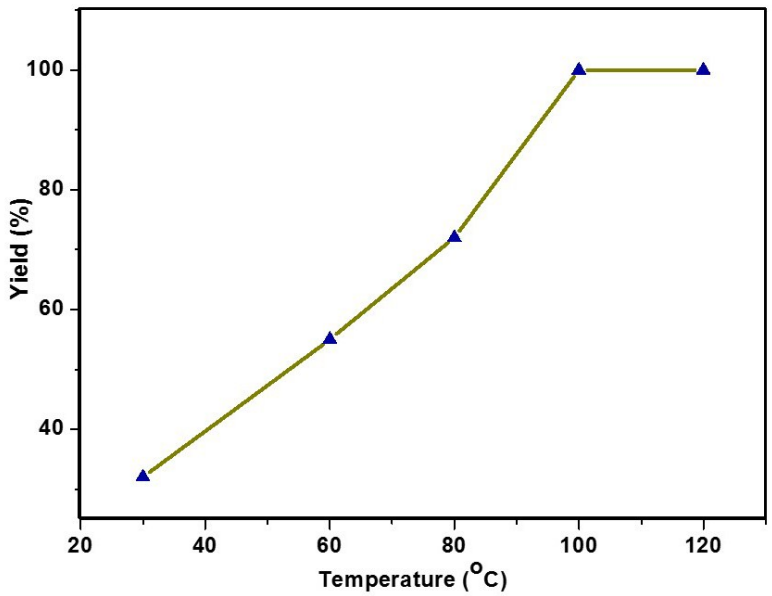

Fig. S15. Effect of temperature on CO_2 cycloaddition reaction at constant pressure (1 bar) and time (8h).

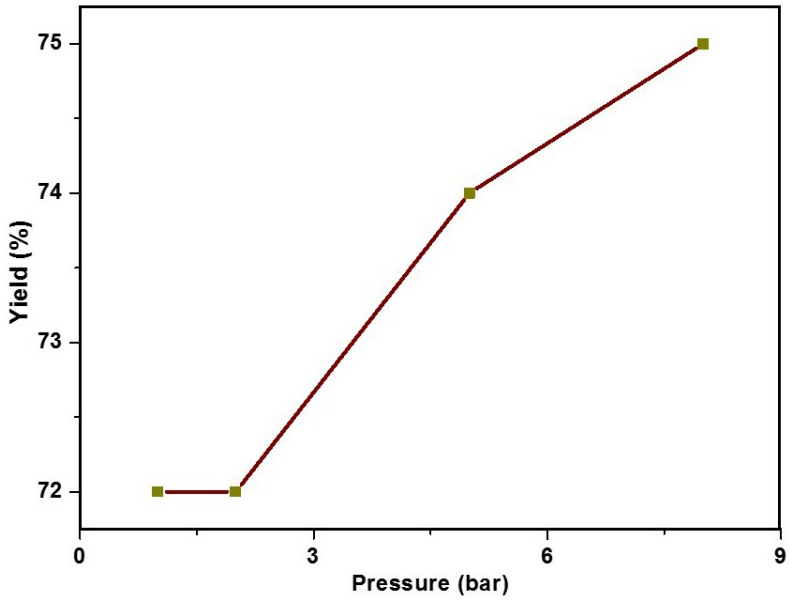

Fig. S16. Effect of pressure on CO_2 cycloaddition reaction at constant temperature (80 °C) and time (8h).

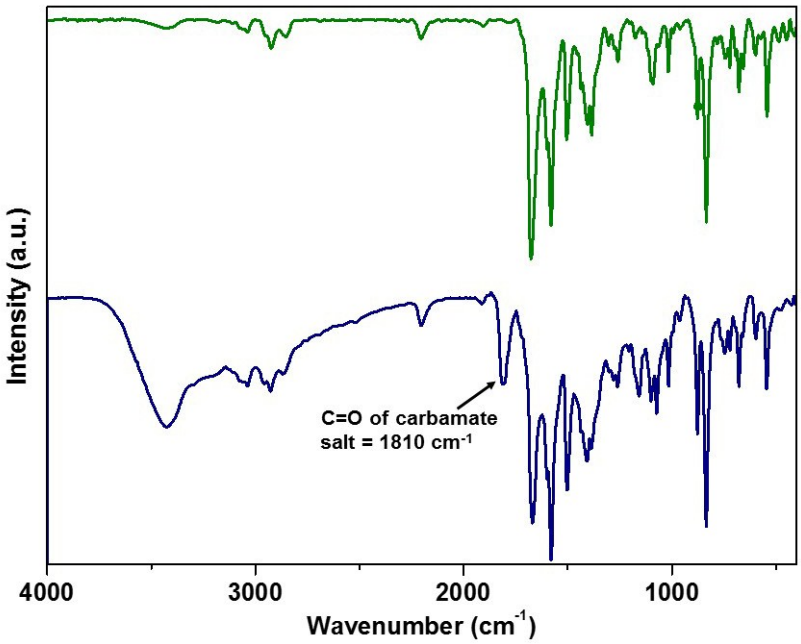

Fig. S17. FT-IR spectra of newly synthesized Co-POP (top) and Co-POP after CO_2 sorption (bottom) indicating the formation of zwitterionic carbamate linkage.

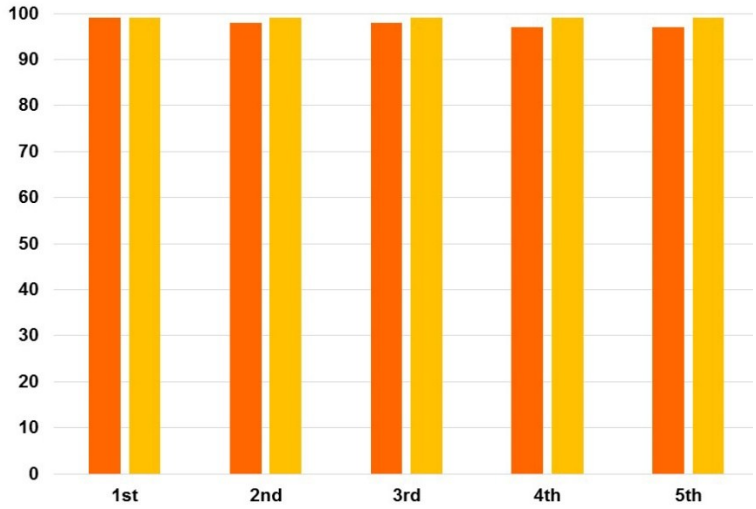

Fig. S18. Recyclability test of Co-POP using conversion of epichlorohydrin as a model. Orange and yellow columns represent product yield and selectivity respectively.

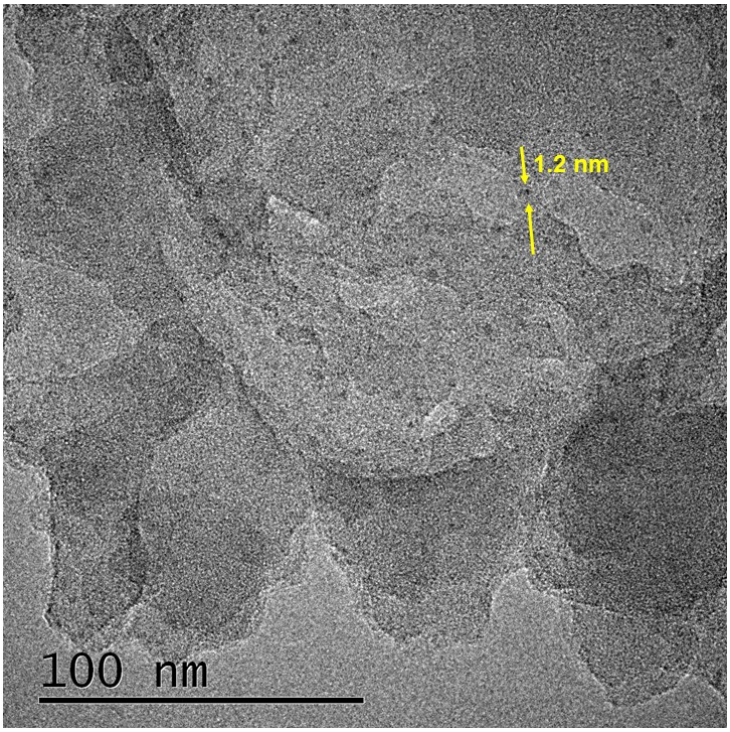

Fig. S19. TEM image of reused catalyst showing ultra-small distribution of metal retained after multiple use.

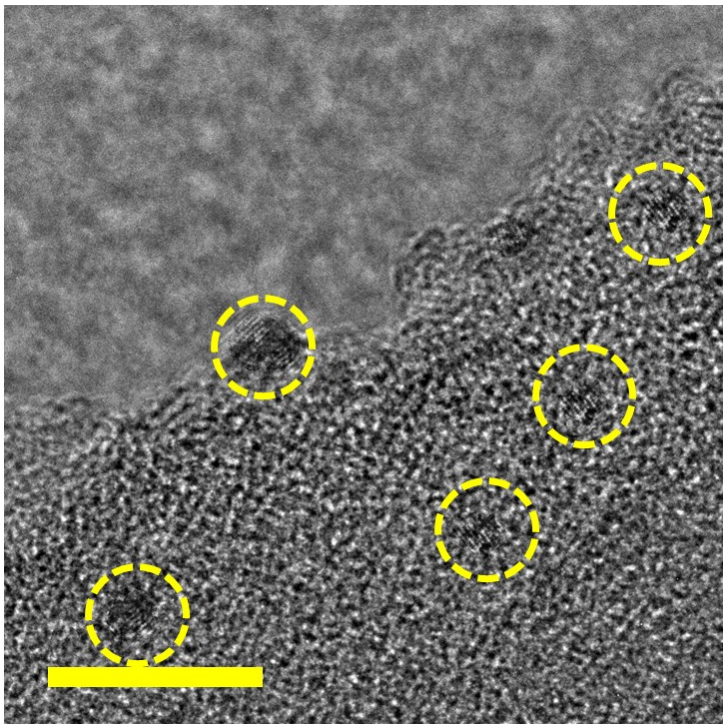

Fig. S20. HRTEM image of the reused Co-POP, scale bar 5 nm.

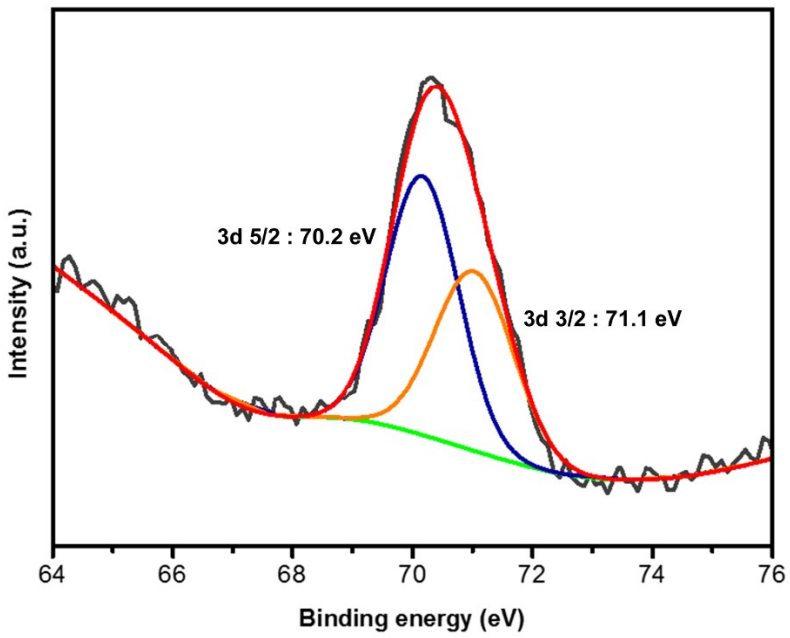

Fig. S21. Br 3d XPS binding energy peak of reused Co-POP.

Table S1. Screening table for the CO_2 cyclization reaction.

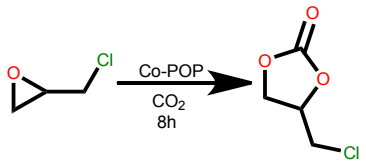

No.	Temp. (°C)	Pressure (bar)	Yield%	Selectivity%
1	120	1	>99	>99
2	100	1	>99	99
3	80	1	72	99
4	60	1	55	99
5	30	1	32	99
6	80	2	72	99
7	80	5	74	98
8	80	8	75	98

Table S2. Control experiments for CO_2 cyclization with different catalysts following standard condition.

No.	Catalyst	Reaction condition	Yield%	Selectivity%
1	Co-POP	Standard	>99	>99
2	Im-grafted POP without Co	Standard	42	92
3	Im-grafted POP without Co	8 bar, 100 °C	48	89
4	Im-grafted POP without Co	1 bar, 140 °C	45	85
5	POP without Co and Im	standard	-	-

Table S3. Table for substrate scope of Co-POP.[a]

Entry	Substrate	Product	Yield	Selectivity	TON[b]	TOF[c]
1	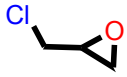	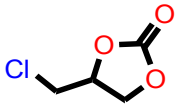	>99	99	1466.7	183.3
2	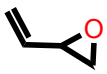	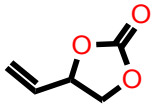	99	99	1466.7	183.3
3	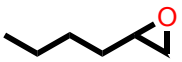	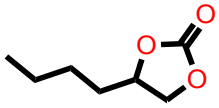	87	98	1288.9	161.1
4	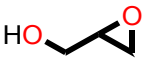	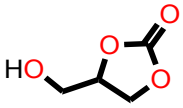	81	97	1200	150
5	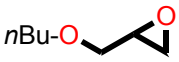	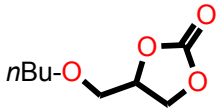	76	99	1125.9	140.7
6	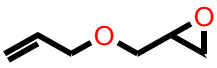	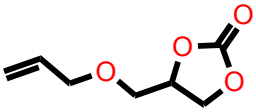	75	99	1111.1	138.9
7	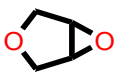	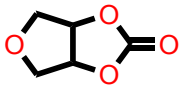	97	99	1437.0	179.6
8		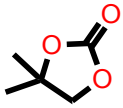	90	95	1333.3	166.7

[a]Standard reaction condition: Co-POP, 20 mg; epoxide, 8 mmol; CO_2 pressure, 1 bar; temperature, 100 °C; reaction time 8h. [b]TON is calculated as mmol of product formed per mmol of catalyst, where mmol of catalyst is calculated based on the Co-content. [c]TOF is calculated as TON/8h (reaction time).

Table S4. Comparison of the catalytic activity of Co-POP with recently reported metal-incorporated POP catalysts.

No.	Epoxide	Catalyst (mg)	Metal content (mg)	Co-catalyst (mol%)	Temp (°C)	Pressure (bar)	Time (h)	Yield%	TOFs (h^{-1})	Ref.
1	Propylene oxide	Zn@SBMMP (20)	3.06	1.8[b]	80	20	4	95	51	S1
2	Propylene oxide	$ZnBr_2$ (10)/HIP-Br-2	0.76	-	25	10	96	99	0.9	S2
3	Propylene oxide	$ZnBr_2$ (1.13)/ polymer	0.33	-	130	10	4	90	64	S3
4	Propylene oxide	Cr-POP (100)	7.12	0.8	100	20	16	98	22	S4
5	Propylene oxide	Co-POP (72)	5.64	0.7	100	20	16	89	20	S4
6	Propylene oxide	Al-CPOP (27)	2.69	-	120	1	24	91	3.8	S5
7	Epichlorohydrin	Cu/POP-Bpy (85)	3.18	3.5	29	1	48	99	4.1	S6
8	**Epichlorohydrin**	**Co-POP (20)**	**0.316**	**-**	**100**	**1**	**8**	**99**	**183.3**	**This work**

5. Discussion on the mechanism:

Based on our proposed reaction mechanism, one may speculate the existence of another reaction pathway where the Im can directly attack the epoxide, and the ring-opened oxide then cyclizes with CO_2. In this case, Im would be the main catalytic site in the POP network, and alteration in reaction conditions (e.g., increasing pressure or temperature) using Co-free Im-grated POP as catalyst should demonstrate a substantial effect. However, no such occurrence was recorded under control experiments (Table S2, Entry 2-4).

It was also necessary to understand whether Br played any role of active co-catalyst in the catalytic protocol. Based on the Br3d XPS pattern, high energy Br $3d_{3/2,}$ and $3d_{5/2}$ peaks can be observed in Co-POP (Fig. S9), inferring that the Br are strongly coordinated to the matrix, i.e. no free-bromides are present in the system. Typically free Br^- produces 3d XPS peaks at ~ 68 eV, which are much lower compared to our case. This, in turn, suggest that it would be energetically unfavorable for those Br to take an active part in the reaction. XPS analysis of the reused catalyst was performed to confer this theory. The Br3d XPS binding energy peaks of the recycled catalyst appeared at the same position as that of the fresh Co-POP (Fig. S21). Moreover, the peak area integration showed a similar area of coverage for both materials. If Br indeed took an active part as co-catalyst in our reaction protocol, an alteration in the spectral pattern should be noticed (e.g., the emergence of a new low energy Br3d peak).

Hence, reckoning the outcomes of these experiments, a conclusion in support of our said mechanistic can be drawn.

6. Referencs:

S1 S. Bhunia, R.A. Molla, V. Kumari, S.M. Islam, A. Bhaumik, *Chem. Commun.*, 2015, **51**, 15732-15735.

S2 J. Li, D. Jia, Z. Guo, Y. Liu, Y. Lyu, Y. Zhou, J. Wang, *Green Chem.*, 2017, **19**, 2675-2686.

S3 J. Wang, J.G. Wei Yang, G. Yi, Y. Zhang, *Chem. Commun.*, 2015, **51**, 15708-15711.

S4 M.H. Alkordi, Ł.J. Weseliński, V. D'Elia, S. Barman, A. Cadiau, M.N. Hedhili, A.J. Cairns, R.G. AbdulHalim, J.-M. Basset, M. Eddaoudi, *J. Mater. Chem. A*, 2016, **4**, 7453-7460.

S5 T.-T. Liu, J. Liang, Y.-B. Huang, R. Cao, *Chem. Commun.*, 2016, **52**, 13288-13291.

S6 Z. Dai, Q. Sun, X. Liu, L. Guo, J. Li, S. Pan, C. Bian, L. Wang, X. Hu, X. Meng, L. Zhao, F. Deng, F.-S. Xiao, *ChemSusChem*, 2017, **10**, 1186-1192.